HTML ABSTRACT * LINKS

Effect of strain-compensation in stacked 1.3 μm InAs/GaAs quantum dot active regions grown by metalorganic chemical vapor deposition

N. Nuntawong, S. Birudavolu, C. P. Hains, S. Huang, H. Xu, and D. L. Huffaker[a]
Center for High Technology Materials, University of New Mexico, 1313 Goddard SE, Albuquerque, New Mexico 87106

(Received 4 February 2004; accepted 11 August 2004)

We have introduced tensile layers embedded in a GaAs matrix to compensate compressive strain in stacked 1.3 μm InAs quantum dot (QD) active regions. The effects of the strain compensation are systematically investigated in five-stack and ten-stack QD structures where we have inserted $In_xGa_{1-x}P$ (x=0.30 or 0.36) layers. High-resolution x-ray diffraction spectra quantify the overall strain in each sample and indicate >35% strain reduction can be accomplished. Both atomic force and transmission electron microscope images confirm that strain compensation improves material crystallinity and QD uniformity. With aggressive strain compensation, room temperature QD photoluminescence intensity is significantly increased demonstrating a reduced defect density. © *2004 American Institute of Physics*. [DOI: 10.1063/1.1805707]

Quantum dot (QD) material has drawn considerable interest for more than ten years due to the optoelectronic advantages that zero-dimensional systems offer. Impressive properties such as low threshold current[1] and current density,[2] low chirp,[3] and high characteristic temperature[4] have been demonstrated. However, low gain at the ground state transition is often considered a limiting factor in the QD device performance.[5] Several groups have reported stacking the QD layers to increase modal gain near 1.3 μm[6–8] resulting in ground-state lasing and larger T_0. However, accumulated overall strain in the epitaxial material can cause defects and nonradiative recombination centers that increase the threshold current density[6] and cause device failure. A thick spacer (300–500 Å) between the QD layers is often used to reduce strain accumulation and defects. However, the extended active region reduces the optical overlap and is not attractive for microcavity lasers.

The compensation of compressive strain by inserting tensile layers has been demonstrated using InGaP and InGaAsP in multiple strained quantum well lasers. Improvements in both crystalline quality and lasing performance including higher photoluminescence (PL) intensity, narrower PL linewidth, and lower threshold current density have been proven.[9–11] The use of strain compensation (SC) to reduce defect formation in stacked QD actives may be a powerful parameter in designing laser structures, but has not been well studied. This is likely due to the inconvenience of a pyrophoric phosphide source in QD-growing molecular beam epitaxy systems. Only recently, the use of tensile GaNAs cap layers[12,13] was reported to improve luminescence efficiency in In(Ga)As-based QDs.

In this letter, we discuss the effects of InGaP SC layers on five-stack and ten-stack QD ensembles. Our samples are grown by metalorganic chemical vapor deposition (MOCVD) at 60 Torr using trimethylgallium (TMGa), trimethylindium (TMIn), tertiarybutylphoshine (TBP), and arsine (AsH_3). Growth is initiated on a GaAs(001) substrate with a 3000 Å GaAs layer at 680 °C, then the temperature is reduced and stabilized for active region growth within the range of 450–520 °C. All active regions consist of a 5 monolayer (ML) $In_{0.15}Ga_{0.85}As$ buffer layer, a 3 ML InAs QD coverage, and a 25 ML $In_{0.15}Ga_{0.85}As$ cap. A postnucleation AsH_3 pause[14] is used after the growth of each QD layer to reduce the defect density. The stacked QD layers are separated by an 8 nm GaAs barrier sandwiching the 8 ML $In_xGa_{(1-x)}P$ SC layer. The SC layer thickness (8 ML) and interface region (2 ML) are measured from high resolution transmission electron microscopy (TEM) images. The interface regions, GaAs/InGaP and InGaP/GaAs, are optimized through the switching of gas flows to minimize In segregation and As–P interchange.

By varying the In content in the SC layers, we study three types of samples; with no SC, with moderate SC (x=0.36), and with more aggressive SC (x=0.30). The lattice constant of the two $In_xGa_{1-x}P$ compositions are a_0=0.5601 nm(x=0.36) and a_0=0.5576 nm(x=0.30) resulting in a lattice mismatch to the GaAs matrix of −0.86% and −1.31%. The composition and thickness of the InGaP SC layer was calibrated by growing InGaP/GaAs superlattice, and investigated by simulated x-ray diffraction (XRD).

Figure 1 shows a TEM image of a five-stack QD active

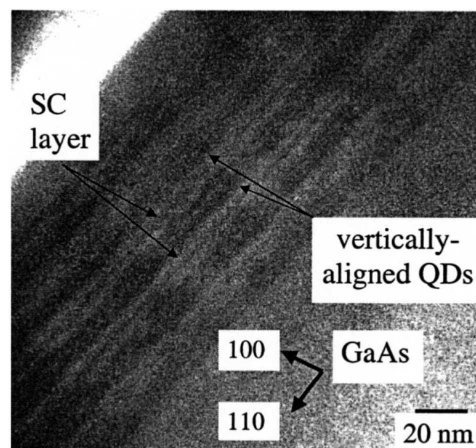

FIG. 1. TEM image of a five-stack QD active with SC layers (x=0.36). The image shows SC layers and vertically aligned QDs.

[a]Electronic mail: huffaker@chtm.unm.edu

 © 2004 American Institute of Physics
Downloaded 12 Aug 2005 to 64.106.37.130. Redistribution subject to AIP license or copyright, see http://apl.aip.org/apl/copyright.jsp

TABLE I. Tabulated XRD data including zero-order peak, total strain, % strain reduction, and FWHM for five-stack and ten-stack samples with no SC and $In_xGa_{1-x}P$ (x=0.36 and 0.30) SC layers.

Data	Five: no SC	Five: x=0.36	Five: x=0.30	Ten: no SC	Ten: x=0.36	Ten: x=0.30
$\Delta\theta$(arcs)	−1962	−1476	−1283	−1602	−1314	−990
$\langle\varepsilon_t\rangle$	0.014 897	0.011 16	0.009 68	0.012 12	0.009 92	0.007 45
Strain reduction (%)	⋯	25	35	⋯	18	38
FWHM (arcs)	320	249	250	748	449	398

with SC layers (x=0.36). The image indicates good crystalline quality and contains several important features such as the vertically aligned columns of strain-coupled QDs, the residual strain field, and the SC layers. The QDs and resulting strain fields appear as large dark ovals. The QD size appears to increase slightly from layer to layer as a result of accumulating compressive strain.

Experimental symmetric scans around (004) reflection in $\omega/2\theta$ geometry are used to measure the effect of SC layers on the strain accumulation and lattice distortion in test structures. Resulting data are summarized in Table I for six samples that have either-five-stack or ten-stack actives with no SC, x=0.36, and x=0.30. Examples of XRD spectra from five-stack structures are shown in Fig. 2 with (a) no SC, (b) x=0.36, and (c) x=0.30. The three spectra are characterized by zero-order peaks located at (a) $\Delta\theta$=−1962 arcsec, (b) $\Delta\theta$=−1476 arcsec, (c) $\Delta\theta$=−1283 arcsec. The zero-order peaks in Figs. 2(b) and 2(c) shift closer to the GaAs substrate peak and indicate reduced compressive strain with decreasing In content in the SC layers. The average perpendicular strain, $\langle\varepsilon_\perp\rangle$ can be determined by[15]

$$\langle\varepsilon_\perp\rangle = \frac{\sin\,\theta_B}{\sin(\theta_B+\Delta\theta)} - 1, \tag{1}$$

where θ_B is the Bragg angle of the GaAs substrate. From Eq. (1) and experimental values for $\Delta\theta$, we calculate the total strain in each sample and list them in Table I. For the five-stack, the total strain, $\langle\varepsilon_\perp\rangle$, varies from 0.014 897 (no SC) to 0.009 68(x=0.30). These strain values indicate a 25% and 35% reduction in compressive strain due to the SC layers compared to the sample without SC layers. Similar XRD data for the ten-stack actives are listed in Table I and indicate less strain than the five-stacks because of partial relaxation due to defect formation.

Improved crystalline quality is evident in the narrowing full width at half-maximum (FWHM) of the zero-order peaks in Figs. 2(a)–2(c). The FWHM decreases from (a) 320 arcsec to (c) 250 arcsec indicating a more uniform distribution of vertical lattice constants. The ten-stack samples indicate significant improvement with SC layers: the FWHM ranges from 748 arcsec without SC layers to 398 with SC layer (x=0.30). An increase in the small oscillation fringe intensity suggests improved crystalline quality with the SC layer. To confirm the reduction of dislocations, another scan using a narrow slit (1.5 mm) was placed in front of the x-ray

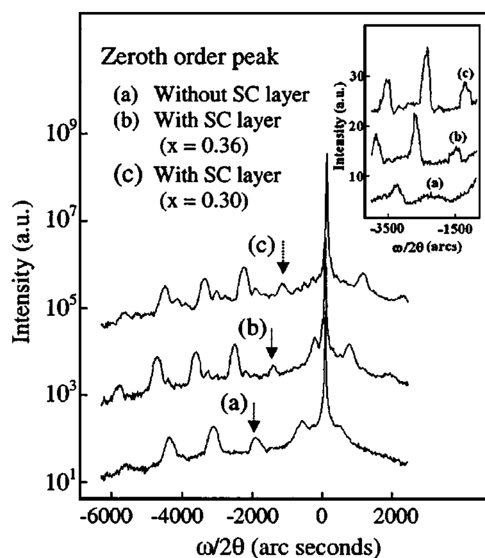

FIG. 2. Symmetric 004 x-ray diffraction patterns for a five-stack QD structure with (a) no SC layer, (b) SC layer (x=0.36), and (c) SC layer (x=0.30). Inset shows the linear scale spectra of a scan run with the insertion of a narrow slit in front of the detector.

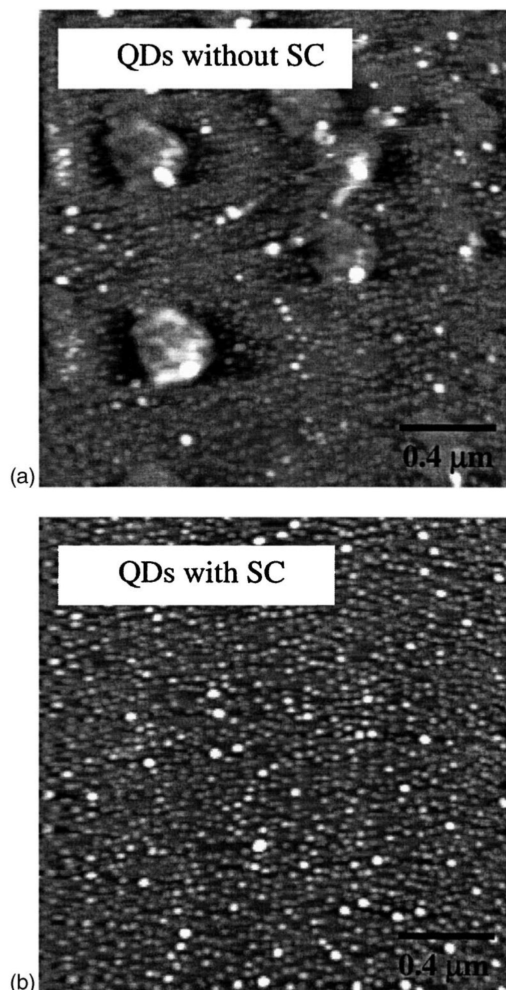

FIG. 3. AFM images (2.0 μm × 2.0 μm) of the second layer for stacked QD (a) without SC layer, (b) with SC layer (x=0.30).

Downloaded 12 Aug 2005 to 64.106.37.130. Redistribution subject to AIP license or copyright, see http://apl.aip.org/apl/copyright.jsp

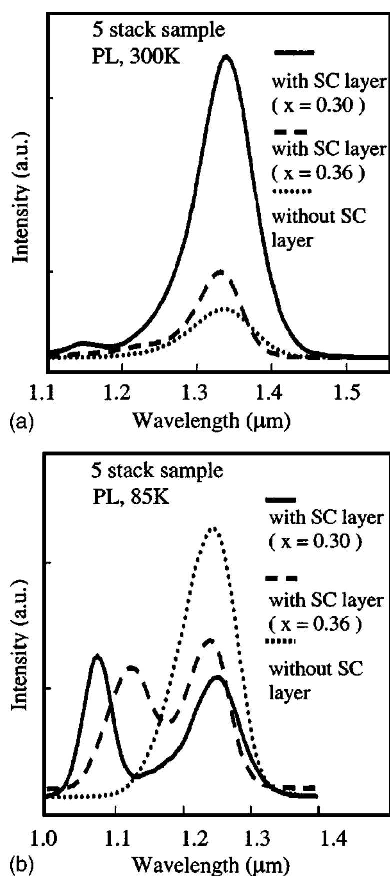

FIG. 4. PL spectra comparing QD active regions with and without SC layers in five-stack sample at (a) 300 K, (b) 85 K.

detector to remove scattering due to dislocations. The diffraction peak intensity with the SC layer ($x=0.30,0.36$) was found to be higher than without SC approximately by factor of 3 from linear scale plot as shown in inset of Fig. 2.

Figure 3 shows atomic force microscope images ($2\ \mu m \times 2\ \mu m$) of the top QD layer in a two-stack active region both (a) without and (b) with $In_{0.30}Ga_{0.70}P$ SC layers. The two-stack without SC has many defects and surface undulations due to the accumulation of compressive strain. The addition of SC layers in (b) results in significantly higher material quality and a QD ensemble with low defect density. From Figs. 3(a) and 3(b), we calculate a QD density of 3 and $4.5 \times 10^{10}/cm^2$ respectively. Average QD height in (a) without SC is ~6 nm, while (b) with SC exhibits a bimodal height distribution centered at both 4 and 6 nm. The QDs in both samples had diameters in the range of 30–40 nm. Further studies are under way to explain and quantify the mechanism for the bimodal QD distribution seen with the insertion of SC layers.

Figures 4(a) and 4(b) show room temperature PL and low temperature PL for five-stack structures both with (dashed) and without (solid) SC layers. The emission wavelengths at room temperature are observed between $\lambda = 1340$ nm and $\lambda = 1325$ nm. A comparison of the five-stack PL spectra in Fig. 4(a) shows the PL intensity with SC is increased by a factor of $1.8(x=0.36)$ and $6.2(x=0.30)$ compared to the uncompensated sample as a result of fewer nonradiative recombination centers. The FWHM varies slightly from sample to sample within a range of 58–70 meV.

The spectra in Fig. 4(b), measured at 85 K, show two distinct peaks in the samples with SC layers that result from the bimodal QD height distribution discussed earlier. The separation between these peaks are 101 and 157 meV for $x = 0.36$ and 0.30, respectively. Only the emission from the larger QDs is visible at room temperature because carriers can freely tunnel from smaller QDs to larger QDs.[16] At low temperature carriers are confined in both the small and large QDs giving rise to two PL peaks.

In conclusion, we have characterized the effect of SC layers in multiple stacked InAs QD structures grown by MOCVD. Our structures are comprised of very thin InGaP SC layers (2 nm) in 8 nm GaAs barriers for SC in five-stack and ten-stack QD actives. From XRD characterization, the SC layers reduce the cumulative strain in a five-stack by over 35%. The reduced overall strain leads to reduced nonradiative recombination centers and greatly improved PL properties in both the five-stack and ten-stack structure. The data suggest that SC layers may be used to improve the performance of stacked QD actives in lasers by increasing internal efficiency and reducing threshold current density.

[1]A. Stintz, G. T. Liu, H. Li, L. F. Lester, and K. J. Malloy, IEEE Photonics Technol. Lett. **12**, 591 (2000).
[2]G. Park, O. B. Shchekin, D. L. Huffaker, and D. G. Deppe, Appl. Phys. Lett. **73**, 3351 (1998).
[3]X. Huang, A. Stintz, H. Li, L. F. Lester, C. Julian, and K. J. Malloy, Appl. Phys. Lett. **78**, 2825 (2001).
[4]O. B. Schekin and D. G. Deppe, Appl. Phys. Lett. **80**, 3277 (2002).
[5]D. Bimberge, M. Grundmann, and N. N. Ledenstov, *Quantum Dot Heterostructures* (Wiley, New York, 1999).
[6]F. Klopf, R. Krebs, J. P. Reithmaier, and A. Forchel, IEEE Photonics Technol. Lett. **13**, 764 (2001).
[7]Y. Qiu, P. Gogna, S. Forouhar, A. Stintz, and L. F. Lester, Appl. Phys. Lett. **79**, 3570 (2001).
[8]H. Chen, Z. Zou, OB Shchekin, and D. G. Deppe, Electron. Lett. **36**, 1703 (2000).
[9]B. I. Miller, U. Koren, M. G. Young, and M. D. Chien, Appl. Phys. Lett. **58**, 1952 (1991).
[10]G. Zhang and A. Ovtchinnikov, Appl. Phys. Lett. **62**, 1644 (1993).
[11]P. J. A. Thijs, L. F. Tiemeijer, J. J. M. Binsma, and T. van Dongen, IEEE J. Quantum Electron. **30**, 477 (1994).
[12]X. Q. Zhang, S. Ganapathy, H. Kumano, K. Uesugi, and I. Suemune, J. Appl. Phys. **92**, 6813 (2002).
[13]X. Q. Zhang, S. Ganapathy, I. Suemune, H. Kumano, K. Uesugi, Y. Nabetani, and T. Matsumoto, Appl. Phys. Lett. **83**, 4524 (2003).
[14]A. A. El-Emawy, S. Birudavolu, S. Huang, H. Xu, and D. L. Huffaker, J. Cryst. Growth **255**, 213 (2003).
[15]A. L. Gray, Ph.D. dissertation, The American University, 2000.
[16]D. L. Huffaker and D. G. Deppe, Appl. Phys. Lett. **73**, 366 (1998).

Downloaded 12 Aug 2005 to 64.106.37.130. Redistribution subject to AIP license or copyright, see http://apl.aip.org/apl/copyright.jsp